ELSEVIER

Flexible transparent conductors based on metal nanowire networks

Chuan Fei Guo and Zhifeng Ren*

Department of Physics and TcSUH, University of Houston, TX 77204, USA

Few conductors are transparent and flexible. Metals have the best electrical conductivity, but they are opaque and stiff in bulk form. However, metals can be transparent and flexible when they are very thin or properly arranged on the nanoscale. This review focuses on the flexible transparent conductors based on percolating networks of metal. Specifically, we discuss the fabrication, the means to improve the electrical conductivity, the large stretchability and its mechanism, and the applications of these metal networks. We also suggest some criteria for evaluating flexible transparent conductors and propose some new research directions in this emerging field.

Introduction

Flexible transparent electrodes (FTEs) are crucial for flexible photoelectronics including flexible organic light-emitting diodes (OLEDs), flexible solar cells, touch screens, wearable devices, and electronic skins [1–6]. Conductors are typically neither transparent nor flexible, while transparent materials are often not conducting. Transparent conducting oxides (TCO) such as indium tin oxide (ITO) are very transparent due to the wide band gap, and are also conducting because of the donor level close to the conduction band [7]. ITO films have dominated the field of photoelectronics for several decades. However, TCO materials are brittle and they often break or form cracks at small strains [8], such that they cannot be used in flexible photoelectronics where folding, stretching, twisting, or serious bending is required. Percolating networks of carbon nanotubes (CNTs) were studied for using as FTEs several years ago [9–12]. However, CNT percolating networks do not possess a low sheet resistance (R_{sh}) and a high transmittance (T) simultaneously. For example, the spray-coated CNT films exhibited a R_{sh} of 328 Ω/□ at a T of 79% [2]. And to achieve a R_{sh} of less than 10 Ω/□, the CNT films require a thickness of more than 100 nm for which the transparency is quite limited [13]. A ratio of direct current conductivity to optical conductivity, σ_{dc}/σ_{op}, is often used as a figure of merit to evaluate the properties of a transparent electrode. Higher σ_{dc}/σ_{op} indicates combined higher transmittance T and lower sheet resistance R_{sh}. The relationship among T, R_{sh}, and σ_{dc}/σ_{op} is [10,14,15]

$$T = \left(1 + \frac{Z_0}{2R_{sh}}\frac{\sigma_{op}}{\sigma_{dc}}\right)^{-2} \quad (1)$$

where Z_0 is 377 Ω, the impedance of free space. However, the direct relationship among σ_{dc}/σ_{op}, T and R_{sh} seems not straightforward. Therefore to evaluate the properties of a transparent electrode, it is much simple by just comparing the transmittance and sheet resistance with commercial ITO films, which exhibit either R_{sh} = ~10 Ω/□ @ T = 80%, or R_{sh} = ~100 Ω/□ @ T = 90% in visible range [16,17]. Any transparent conductors with properties comparable or better than that of ITO are potentially useful in industry. CNT films are not comparable to ITO films due to the high nanotube–nanotube junction resistance, as well as the fact that part of the CNTs is semiconducting.

Metals have the best electrical conductivity and can be easily welded together on the nanoscale to eliminate the junction resistance and thus metal nanowire (NW) networks have been used to replace CNT networks. This review summarizes the fabrication, properties including flexibility and its mechanism, and applications of FTEs made of metal NWs. We discuss NW networks made by two routes: bottom up method, solution process to assemble the nanowires into a network, for which a post treatment is often required to weld the contacting nanowires; and top-down method, deposition of a metal film onto a template or a mask to form a fully interconnected network without any wire–wire junction resistance. Such

*Corresponding author:. Ren, Z. (zren@uh.edu)

 http://dx.doi.org/10.1016/j.mattod.2014.08.018

Please cite this article in press as: C.F. Guo, Z. Ren, Mater. Today (2014), http://dx.doi.org/10.1016/j.mattod.2014.08.018

interconnects can be regarded as perforated metal films which exhibit better electrical conductivity and flexibility. In addition, we point out in this review that properties including haze, surface roughness, strain fatigue, adhesion, and stability of an FTE are also important depending on the application, and suggest new criteria considering these properties to properly evaluate FTEs.

Solution processed metal nanowires for FTEs

Percolating Ag NW networks

The first random metal NW network was made of solution processed Ag NWs to replace nanoimprinted metal grid and CNT films as the transparent electrodes [16,18,19]. Figure 1a–c illustrates the Ag NW suspension, scanning electron microscopy image of a Ag NW network, and optical image of a Ag NW network on flexible polyethylene terephthalate (PET) substrate. The Ag nanowires were synthesized by the reduction of Ag nitrate in the presence of poly(vinyl pyrrolidone) (PVP) in ethylene glycol [20]. A suspension of the Ag NWs was drop-casted to the substrate. After drying, a random percolating network of Ag NWs was formed. Such a network often has a large sheet resistance (R_{sh} = ~1 kΩ/□) as a result of the large wire–wire junction resistance and a comparable transmittance to that of ITO films [16]. The junction resistance can be as large as 1 GΩ due to a thin PVP layer coating on the surface of Ag nanowires (Fig. 2a) [21], and eliminating this resistance is an effective way to improve the electrical conductivity of the metal NW network FTEs (Fig. 2b–h). The PVP layer can be removed by annealing (typically at 200°C for 20 min), leading to direct contact and welding of NWs (Fig. 2b) [16]. However, for FTEs, the substrates are typically polymers which cannot survive under high temperature annealing. To solve this problem, several other methods avoiding high temperature were developed. The Cui group electrochemically coated a thin Au film (Fig. 2h) on the Ag nanowire networks, reducing the junction resistance from ~1 GΩ to ~450 Ω and R_{sh} to less than 100 Ω/□ [21]. Gannet et al. used laser illumination to cause local temperature rising around the junctions, resulting in plasmonic welding (Fig. 2g) which effectively increase the electrical conductivity by three orders of magnitude [22]. Because this process is self-limited, the welding effect is local and does not cause any damage to the other part of the nanowires or significant change of transmittance. The plasmonic-welded Ag NW networks could withstand folding, bending, and even crumpling without significant increase in resistance [22]. Tukono et al. developed a welding process by cold pressing at 25 MPa for 5 s. The Ag nanowires were well joined, and unlike the methods above, all the nanowires including the joints were in the same plane, such that the surface roughness of the FTEs is much smaller (Fig. 2d). Ag nanowire networks made with this process achieved a R_{sh} of 8.6 Ω/□ at a transmittance of 80%. The sheet resistance of the regular post-annealed Ag NW electrodes increased by more than six-fold after only 100 bending cycles with a curvature radius of 5 mm. By contrast, the sheet resistance of mechanically pressed Ag NW electrodes maintained its low sheet resistance, with a small increase of less than 19% even after 1000 cycles of bending due to the strong welding between NWs [23]. Lee et al. showed that R_{sh} of a Ag nanowire network could be significantly reduced by solvent washing (for removing the PVP) of the Ag nanowires followed by a spray process (Fig. 2f) instead of applying drops, without any post-treatments. Such Ag NW networks exhibited a R_{sh} of 18.9 Ω/□ at a T of 94% which is better than the results with post-annealing, together with a lower strain fatigue [24].

It is worth pointing out that the data in different references mentioned above may not be compared because the data are affected by the nanowire length and diameter, which were different in different reports. To this point, Lee et al. developed a multicycle growing method to produce 'very-long Ag nanowires' with an average length of ~100 μm, much longer than the Ag nanowires made by one-time growth (<20 μm). With a sheet resistance of 9 Ω/□, the network exhibited a transmittance of 89%, superior to that of the counterpart using common shorter nanowires (69%) [25]. Electrodes with longer nanowires exhibited excellent flexibility: no increase of resistance was seen after 10,000 cycles of bending at a bending radius of 2 mm [25].

Some recent theoretical and experimental results show that for stick networks, the sheet resistance decreases with increase of length to diameter ratio (L/D), or fraction of long sticks, or area fraction (AF) of the metal, or the decrease of junction resistance [15,26–28]. For stick networks with fixed L/D and junction resistance, increasing AF (above the percolation threshold) will lead to increasing of electrical conduction and decreasing of optical transmittance. With larger L/D or smaller junction resistance, we can decrease AF to some extent and hence increase the transmittance.

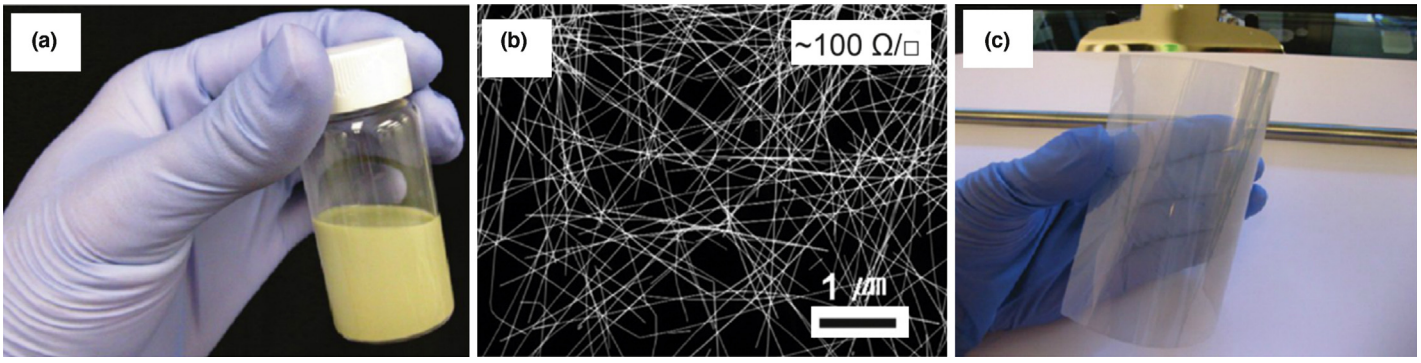

FIGURE 1

Solution processed Ag NW networks for FTEs. (a) Ag nanowire suspension. (b) Scanning electron microscopy (SEM) image of a Ag NW network. (c) Optical image of a Ag NW network on flexible polyethylene terephthalate (PET) substrate. Figures reprinted with permission from Ref [21]. Copyright American Chemical Society 2010.

Please cite this article in press as: C.F. Guo, Z. Ren, Mater. Today (2014), http://dx.doi.org/10.1016/j.mattod.2014.08.018

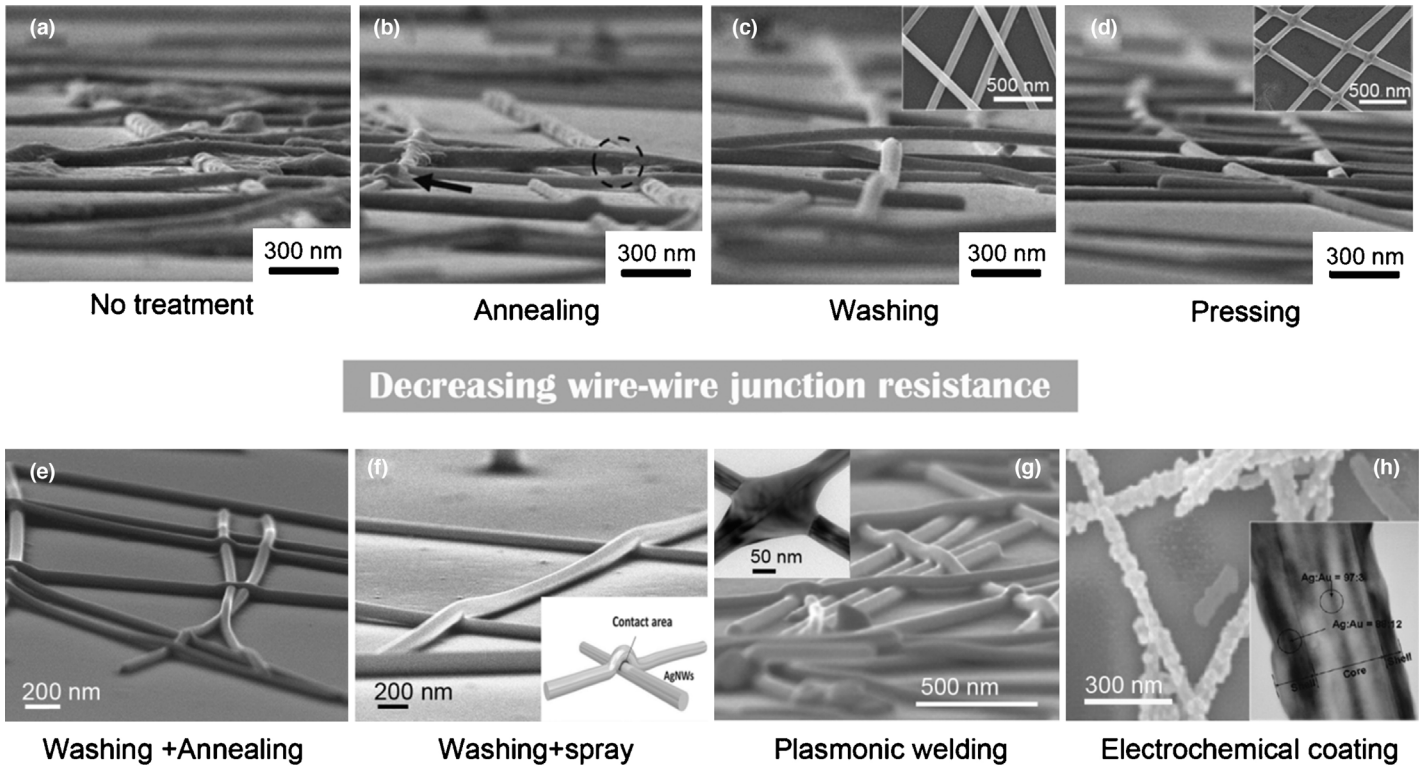

FIGURE 2

Different methods for decreasing wire–wire junction resistance of Ag NW networks. (a) Ag NW network without post treatment, showing residue and loosely contacted junctions. (b) Thermal annealed Ag NW networks, showing Ag residue indicated by the arrow and welding indicated by the dashed circle. (c) Removing the PVP layer on the Ag NW surfaces, inset is a plan view. (d) Washing the NWs followed by pressing the network, showing good connection and small roughness, inset is a plan view. (e) Washing the NWs plus annealing, showing no residues on Ag NW surfaces. (f) Washing plus spray, inset is a schematic illustration of a wire–wire junction. (g) Light induced plasmonic welding, inset is a transmission electron microscopy (TEM) image of a welded junction. (h) Ag NW networks with electrochemical-deposited Au film, inset is a TEM image of Au coated Ag NW. Figures reprint with permission from Ref [23] (panels a–d), copyright Springer 2011, Ref [24] (panels e,f) copyright Wiley VCH 2013, Ref [22] (panel g) copyright Nature Publishing Group 2012, and Ref [21] (panel h) copyright American Chemical Society 2010.

According to van de Groep et al.'s simulation [29], for a Ag network with wire width from 45 nm to 110 nm, transmittance is close to ~1.1 times of normalized clear aperture ($1 - AF$) as a result of the fact that the subwavelength NWs can strongly scatter light. Bergin et al. suggested $T = 1 - 0.87AF$ for Ag NW networks with a diameter of 40 nm [26], and when the junction resistance is fixed to 2 kΩ, L/D should be larger than 400 in order to achieve a combined property of $T > 90\%$ and $R_{sh} < 100\ \Omega/\square$ [27].

Cu and Au nanowire percolating networks

Apart from Ag, nanowires of other metals like Cu and Au were also studied for FTEs. Cu has the best electrical conductivity but much lower price compared with Ag and Au. Wiley et al. showed that Cu nanowires could grow from spherical Cu seeds in an aqueous solution of NaOH, ethy-lenediamine, $Cu(NO_3)_2$ and hydrazine [30–33]. Networks of Cu NWs (10 μm in length and 90 nm in diameter) had a sheet resistance of 15 Ω/□ and a transmittance of 65%, which were not as good as Ag nanowire networks or ITO films, but the transmittance was 15% higher than CNT networks [31]. The relatively low transmittance should be related to the small aspect ratio of the NWs. With 28.4 μm long and 75 nm thick NWs (Fig. 3a), R_{sh} can be 60 Ω/□ @ $T = 94.4\%$. This is close to the properties of ultralong (up to 40 μm) and fine (16.2 nm) Cu NW networks which exhibit a R_{sh} of 51.5 Ω/□ @ $T = 93.1\%$ [34]. The Cu nanowire FTEs did not show fatigue by bending to a 2.5 mm radius for 1000 cycles under both tension and compression [31]. However, Cu NWs are not stable in air. At a temperature of 85°C, resistance of Cu NW networks increased one order of magnitude in just one week (by contrast, to increase the same value Ag NW networks needed ~2 weeks). This problem could be solved by introducing a protective coating like Ni [33]. Figure 3a,b shows SEM images of Cu NW network before and after coating with a Ni layer, respectively. And Fig. 3c clearly exhibits that the NW is a Cu-core/Ni-shell structure. Cupronickel (Cu-Ni) nanowire networks did not exhibit apparent change of resistance in an 85°C atmosphere for 30 days (Fig. 3e), however, the incorporation of Ni reduced the electrical conductivity of the network as Ni is not as conducting as Cu (Fig. 3d) [33].

Au is an excellent conductor with conductivity close to Cu and Ag, and is much more stable. But Au is not easy to form NWs with size similar to that of Ag NWs by using a solution chemical reaction. Yang et al. synthesized Au NWs with a diameter of 1.6 nm and a length of several microns by reducing $HAuCl_4$ with oleylamine [35], and Sanchez-Iglesias et al. applied a monolayer of these ultrathin Au NWs as a transparent electrode. The monolayer exhibited a sheet resistance of 400 Ω/□ at a high transmittance of 96.5% [36]. Note that such a monolayer is not a network; instead it was made of well-aligned Au NWs with a ~1 nm gap. The flexibility of this Au nanowire monolayer was not discussed but is expected to be quite good due to the ultra-large aspect ratio.

Please cite this article in press as: C.F. Guo, Z. Ren, Mater. Today (2014), http://dx.doi.org/10.1016/j.mattod.2014.08.018

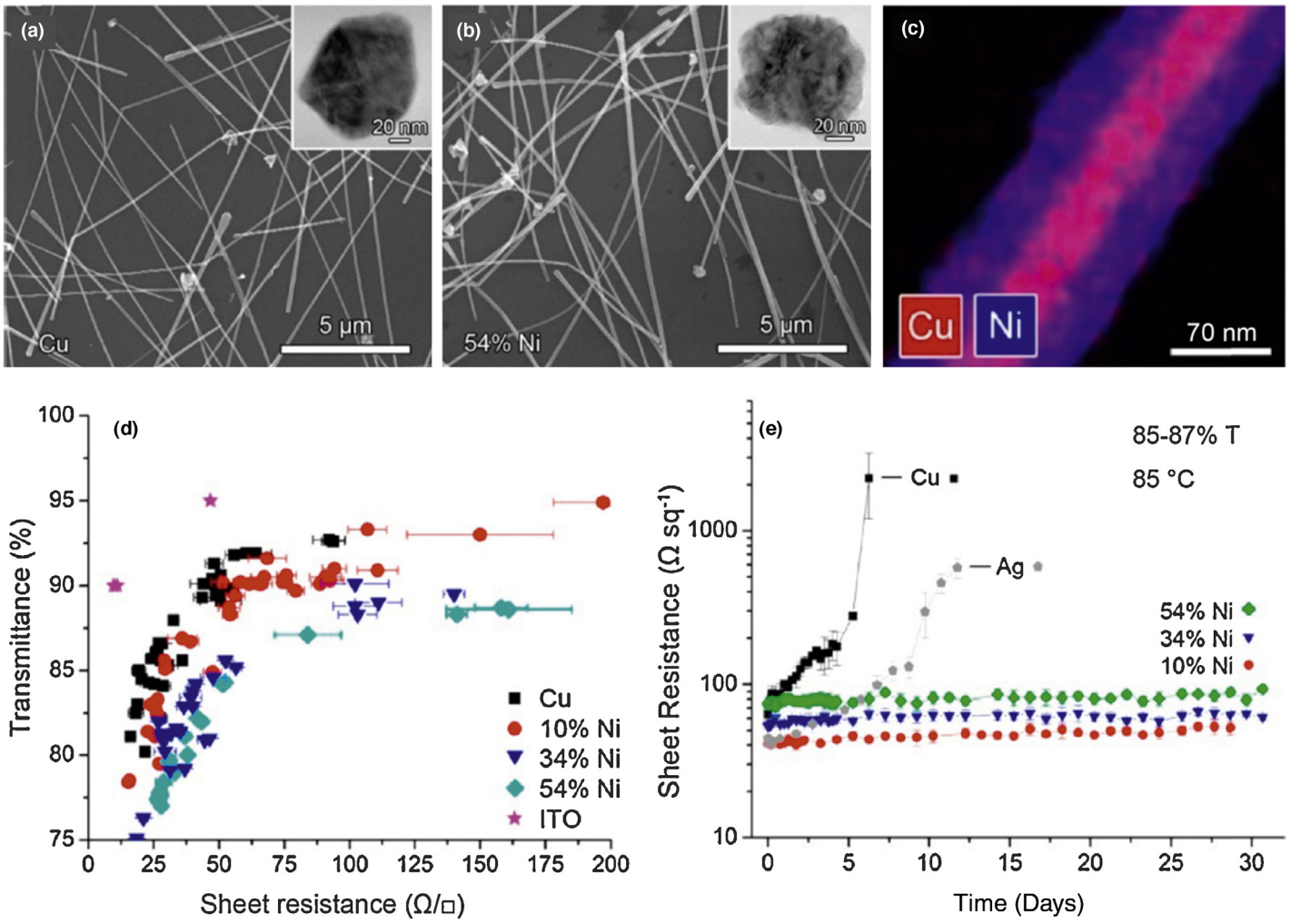

FIGURE 3

Cu and Cu-Ni NW networks. (a) SEM image of a Cu NW network. Inset is a TEM image of the cross-section of a Cu nanowire. (b) SEM image of a Cu-Ni (54% concentration) NW network, and inset is a cross-section TEM image of a Cu–Ni NW. (c) Energy dispersive X-ray spectroscopy image of a Cu-Ni NW. (d) The comparison of transmittance and sheet resistance of ITO film, Cu, and Cu-Ni NW networks with difference content of Ni. (e) The thermal stability of Cu, Ag, and Cu-Ni NW networks with different content of Ni. Figures reprinted with permission from Ref [33], copyright American Chemical Society 2012.

Another type of Au nanowires was made by using electrodeposition. The diameter of the nanowires was 47 nm and length < 6 μm. The electrodeposited Au NW networks exhibited a R_{sh} of 49 Ω/□ @ T = 83% [14]. The overall performances of the Cu and Au NW electrodes were not as good as Ag NW electrodes, and mechanical properties were not extensively investigated, and few measures were carried out to reduce the junction resistance.

Flexible, transparent, and conducting composites based on solution processed metal nanowires

The resistance of metal nanowire networks can be reduced by introducing two-dimensional flakes of graphene or graphene oxide, or by burying or mixing the metal nanowires in polymers like insulating polyvinyl alcohol (PVA), and conducting poly(3,4-ethylenedioxythiophene) poly(styrene sulfonate) (PEDOT:PSS). Lu et al. first buried Ag NWs into PVA to decrease the surface roughness (roughness from 75 nm for Ag NWs on PET to 1.27 nm for buried Ag NWs). The electrode showed a R_{sh} of 63 Ω/□ @ T = 87.5%, and could be folded with a curvature of 100–200 μm [37]. Peumans et al. showed that besides small roughness, PEDOT:PSS/Ag NWs had superior electrical conductivity and mechanical properties to ITO on plastic and improved efficiency in flexible organic solar cell using these composites [38]. Liu et al. showed that a Ag NW network covered with a layer of graphene showed a decrease of T of only less than 5%, but several times enhancement of electrical conductivity and significantly decreased surface roughness [39]. Pei et al. showed that graphene oxide (GO)-soldered Ag NW network exhibited a R_{sh} of 14 Ω/□ with 88% transmittance at 550 nm, and large stretchability up to 130% [40]. The GO/Ag NW network exhibited a decreased R_{sh} (up to 53%) and improved chemical, light, and thermal stabilities [41]. In brief, the composite materials improve the electrical property of the FTEs either by better welding of nanowire junctions, or by offering new paths for carrier transport, and can also decrease the surface roughness.

Fully interconnected networks made by vacuum deposition: a top-down method

The most ideal percolating networks should have zero junction resistance – a perforated flat metal film. This can be easily realized

Please cite this article in press as: C.F. Guo, Z. Ren, Mater. Today (2014), http://dx.doi.org/10.1016/j.mattod.2014.08.018

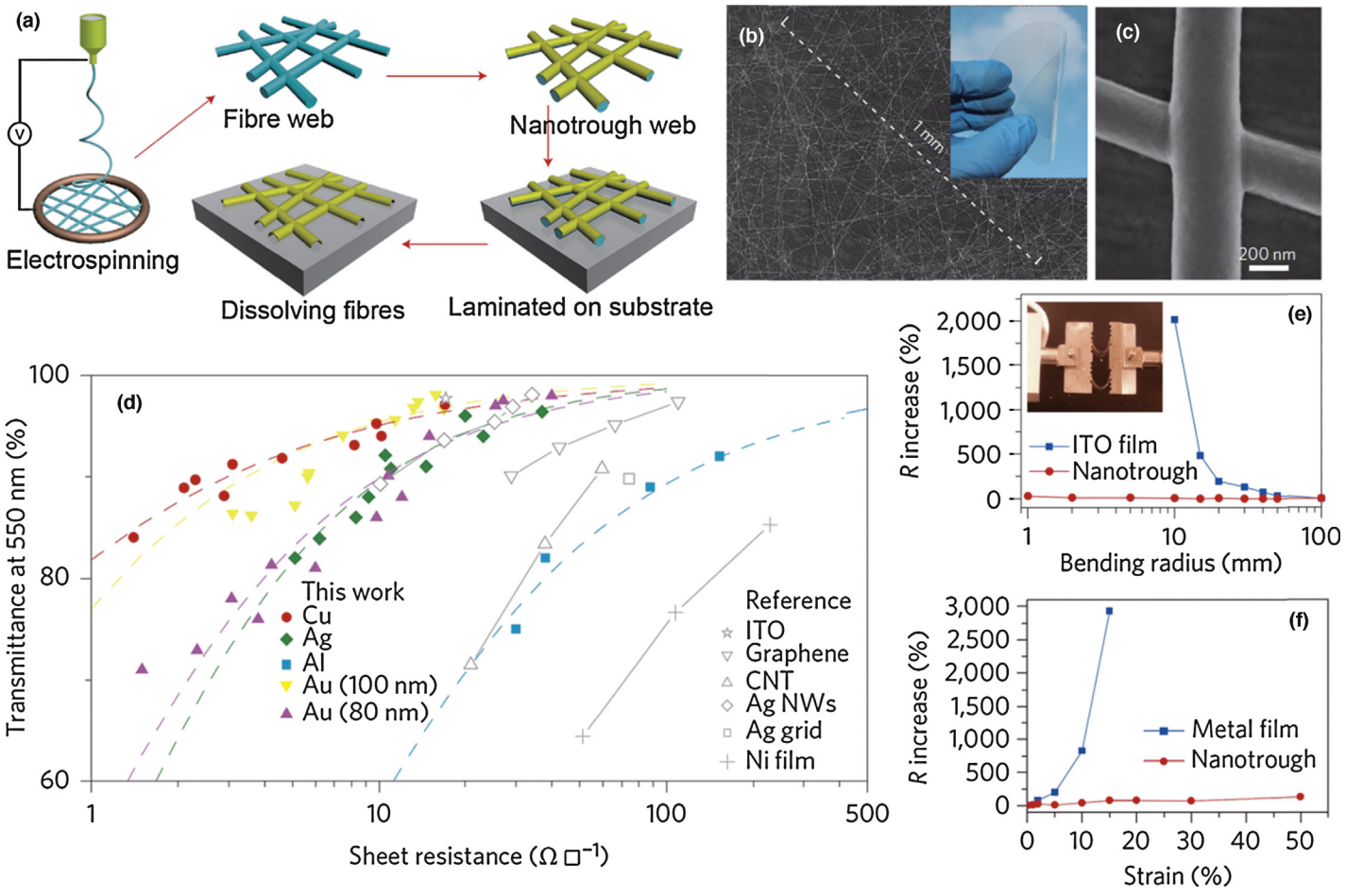

FIGURE 4

Highly transparent and conducting nanotrough networks. (a) Schematic illustration of the fabrication of metal nanotrough networks. (b) Plan view SEM image of a nanotrough, inset is an optical image of a metal nanotrough network on PET. (c) High magnification SEM image of a junction. (d) Sheet resistance and transmittance of Cu, Ag, Al, and Au nanotroughs, as well as reference transparent electrodes including ITO, graphene, CNT, Ag NW networks, Ag grids, and Ni films. (e) Change of resistance versus bending radius for bendable transparent electrodes consisting of Au nanotrough networks or ITO films on 178-mm-thick PET substrates. (f) Change of resistance versus uniaxial strain for a stretchable transparent electrode consisting of Au nanotrough networks on 0.5-mm-thick PDMS substrate. The rapid degradation of a Au thin film with a thickness similar to the nanotroughs (80 nm) is shown. Figures reprinted with permission from Ref [42], copyright Nature Publishing Group 2013.

by using conventional nanofabrication methods. Guo et al. used nanoimprint lithography to make metal grids as the electrodes for organic light-emitting diodes (OLEDs) and solar cell applications [18,19]. The metal grids exhibited transmittance and sheet resistance comparable to ITO films, but potentially better flexibility. However, such an improvement in mechanical properties comes at a price, and is often too expensive for practical applications. In 2013, Cui et al. used electrospun polymer network as the template and deposited a metal film (e.g. Au, Ag, Cu) onto the template, then they removed the polymer template, leaving behind a fully interconnected metal network, which they called nanotrough networks (Fig. 4a) [42]. Corresponding mesh size (M), wire-width (W), and thickness (t) of the nanotrough networks are tens of microns, 420 nm, and 80–100 nm (Fig. 4b), respectively. Because of the good connection between nanotroughs (Fig. 4c), the Au nanotrough network achieved a R_{sh} of only 8 Ω/□ @ T = 90%, much better than that of any doped metal oxide films (e.g. ITO), or solution processed metal nanowire networks (Fig. 4d). The nanotrough networks also presented good flexibility (Fig. 4e,f).

Also in 2013, we used a novel method, grain boundary lithography, to make metal nanomeshes by taking full advantage of the interconnectivity of grain boundaries of monolayered metal grains with a size close to 1 μm [43,44]. The fabrication process is shown in Fig. 5. And the metal nanomeshes can be floated on water with a wedging transfer method and then transferred to any substrate. Different from the nanotrough networks, typical mesh size (M), line width (W), and thickness (t) of the metal nanomeshes are only 1 μm, 60 nm, and 35 nm, respectively, and all the NWs are in the same flat plane. For a Au nanomesh with a R_{sh} of 21 Ω/□, the average transmittance in 400–1000 nm is 82.5% [44]. It is expected that both R_{sh} and T can be improved by increasing M, W, and t depending on the requirement of applications. In another work, Han et al. used a spontaneously cracked TiO_2 gel films as the template for making Ag networks. The Ag lines were typically 500–1000 nm wide, and the mesh size was ~20 μm, and thickness was 80 nm. The Ag networks exhibited a R_{sh} of 10 Ω/□ at a transmittance of 88% [45], and very close to the Ag nanotrough networks [42]. It is worth pointing out that the type of metal also affects the

Please cite this article in press as: C.F. Guo, Z. Ren, Mater. Today (2014), http://dx.doi.org/10.1016/j.mattod.2014.08.018

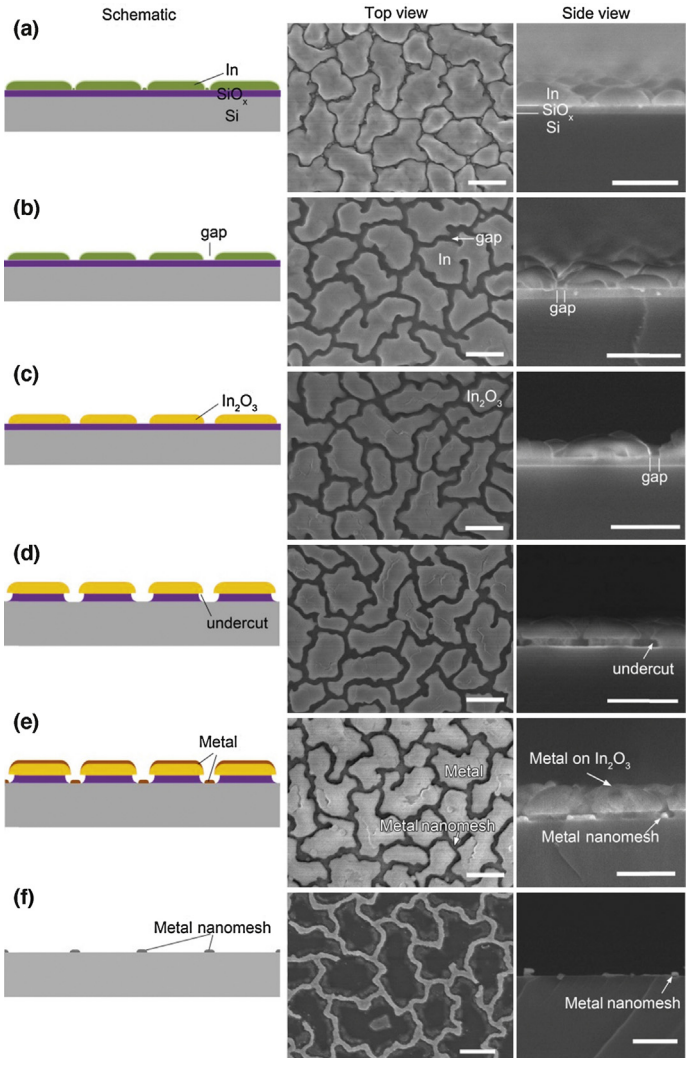

FIGURE 5

Fabrication of metal nanomeshes by grain boundary lithography. The left column represents schematics, while the middle and right columns are corresponding top view and cross sectional SEM images, respectively. (a) Deposition of In/SiO_x bilayer on a Si wafer. (b) Gap formation by etching in diluted HNO_3. (c) Conversion of In islands into In_2O_3 islands by thermal oxidation. (d) Undercut formation by rinsing in diluted HF. (e) Deposition of metal film leading to the formation of metal nanomesh in the grooves. (f) Lift-off process to remove In_2O_3 and SiO_x. Scale bars are 500 nm. Figures reprinted with permission from Ref [44], copyright Nature Publishing Group 2014.

properties. Cu and Au are not as reflective as Ag, such that by replacing Ag with Cu or Au, it is possible to get higher transmittance. This was reflected in Ref [42] that Cu and Au nanotrough networks exhibited performances better than that of Ag. However, the large sizes in nanotrough networks and crack-templated networks, especially the large mesh size, may lead to limited applications. By contrast, the Au nanomeshes show good uniformity of mesh size of only ~1 μm, and can be regarded as flat films suitable for many applications.

The fully interconnected metal networks also present advantage of good flexibility. The R_{sh} of the nanotrough network only increased by 40% when stretched to a 50% strain (Fig. 4f) [44]. The Au nanomesh made by grain boundary lithography had a change of resistance (R/R_0, where R is the measured resistance under stretching and R_0 is the original resistance) of 13.3 and the R_{sh} increased 2.2 times when stretched to 160%, and the R_{sh} did not show any increase until the sample was stretched to 80% (Fig. 6a,b). By stretching to 50% or 100% strain for 1000 cycles, there was a very small increase in resistance after releasing the strain (32% increase for 50% strain cycling, and 70% increase for 100% strain cycling), indicating that fatigue was small (Fig. 6c). Bending to a V-shape was also studied. When bending radius is far smaller than 1 mm, resistance only increased by 54% after 500 bending cycles (Fig. 6d) [44]. No increase of resistance was observed when bending with a radius of 1 mm for more than 1000 cycles. Our recent study showed that cyclic deformation may also lead to recover of pre-damaged Au nanomeshes due to cold-welding of fractured Au nanowires [46]. We pointed out that dimensions of meshes in percolating metal networks affect stretchability. It was shown that larger mesh size to wire-width (M/W) ratio results in much larger stretchability (Fig. 6a,b), and this was proven in a demonstration with coarse and fine ligaments made of paper as shown in Fig. 6e,f.

For the first time, we also systematically studied the mechanism of the large stretchability of fully interconnected metal networks with a deep understanding of the physics [44]. At a relatively small strain (<40%), the Au nanomesh (which is made of interconnected serpentines) deforms elastically (Fig. 7a), and the Au ligaments twist and deflect out of plane to release the stresses (Fig. 7b). While at large strains (>40%), some Au ligaments deform plastically and rupture, forming distributed cracks (Fig. 7c). The distributed rupture results in a larger network such that the electrode can be regarded as a nested self-similar mesh and gives rise to extra stretchability, which has also been proved with a demonstration that a paper mesh structure with pre-cutting cracks is quite stretchable (Fig. 7d). Note that out-of-plane deformation always work during the stretching, no matter distributed rupture happens or not. The distributed rupture of the Au nanomesh is quite similar to the rupture in a continuous Au films deposited on PDMS, which can be stretched to 30% [47,48]. The difference is that in the Au nanomesh the serpentines make the structure much more stretchable [49]. The distributed rupture mechanism also implies that buried metal NW networks may not be very stretchable since the slipping of the nanowires is not allowed.

The underlying PDMS substrate plays two important roles for the large stretchability. First, PDMS is soft, the huge difference in Young's modulus between Au and PDMS allows the Au ligaments to deform out-of-plane. Second, at large strains, the PDMS substrate stabilizes the local cracks and allows elsewhere to rupture, leading to homogeneously distributed cracks [44]. If there is no PDMS substrate, say, for a free-standing Au nanomesh, once a crack is formed, the crack will propagate throughout the mesh and the sample breaks into two halves. Before our work, the function of the flexible substrate for metal nanowire networks was not properly understood. Indeed, the substrate is so important that ITO films, which are brittle, can even be stretched to 30% when deposited on PDMS [8].

The mechanism of the stretchability for the Au nanomesh and solution processed Ag NW networks should be similar in some content. Pei et al. proposed a squashing mechanism for the GO-soldered Ag NW networks, which could be stretched to more than 100% [40]. Pei et al.'s mechanism may explain the deformation at

Please cite this article in press as: C.F. Guo, Z. Ren, Mater. Today (2014), http://dx.doi.org/10.1016/j.mattod.2014.08.018

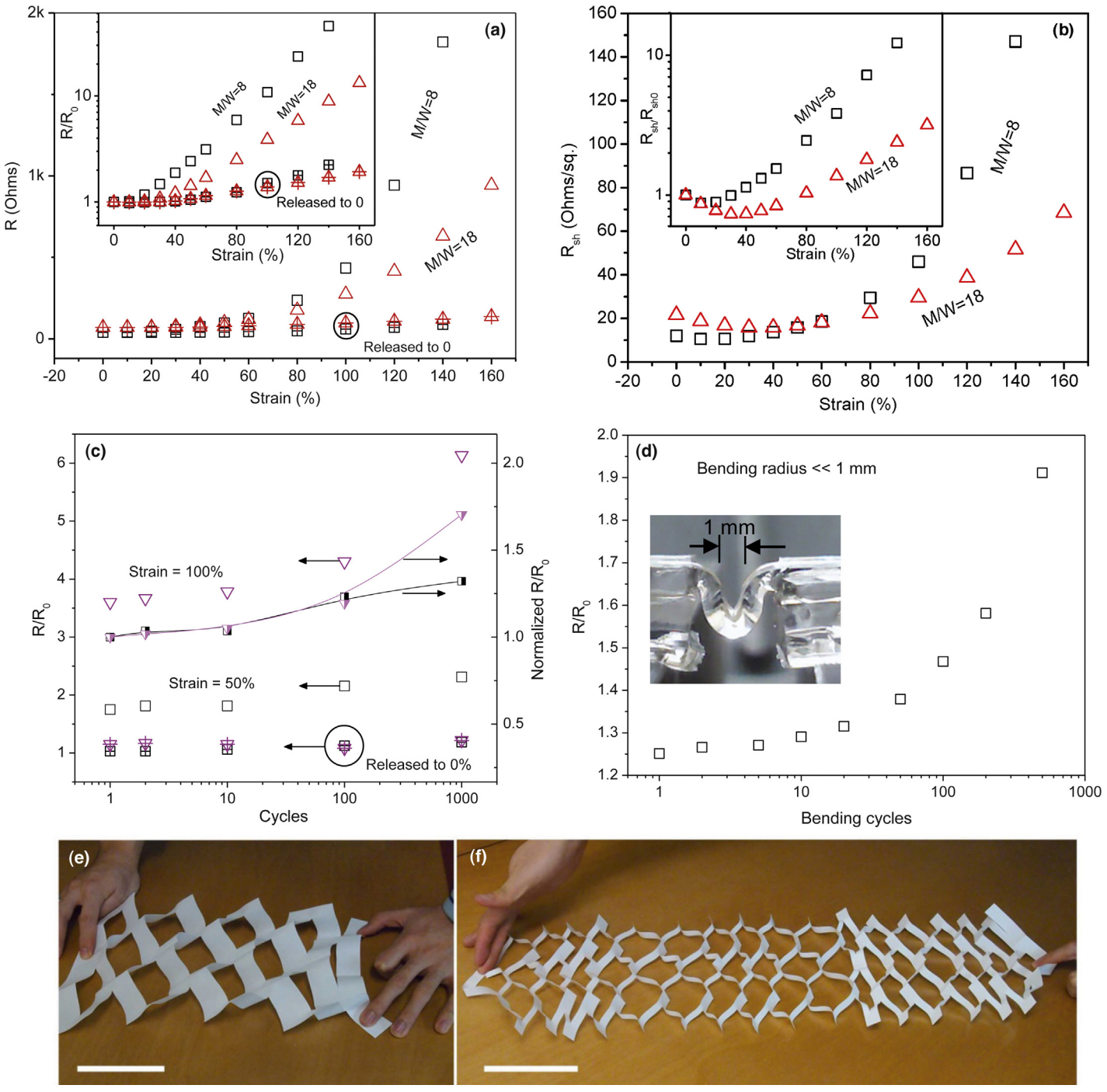

FIGURE 6

Flexibility and resistance of metal nanomeshes. (a) R and R/R_0 (inset) as a function of tensile strain. The Au nanomesh with a mesh-size to line-width ratio (M/W) of 18 (red triangles) has a R/R_0 of only 13.3 as the sample is stretched to a strain of 160%, more stretchable than the one with M/W of 8. (b) R_{sh} and R_{sh}/R_{sh0} (inset) as a function of tensile strain for Au nanomeshes. The sample with an M/W ratio of 18 shows a R_{sh}/R_{sh0} of only 3.2 when stretched to 160%; and R_{sh} is even lower than R_{sh0} below 80% strain. (c) Change in resistance with strain cycles of two Au nanomesh samples with M/W of 18 by stretching to 50% (black symbols) and 100% (purple symbols). (d) R/R_0 as a function of bending cycles. The bending radius is far smaller than 1 mm and sample appears to be a 'V' shape when bent. (e,f) Stretching two sheets of letter-sized papers containing an array of slits with coarse and fine ligaments, respectively. The closely spaced slits appear to be much more stretchable. Scale bars are 10 cm. Figures reprinted with permission from Ref [44], copyright Nature Publishing Group 2014.

small strains. However, there should be out-of-plane deformation of the Ag NWs (but the deformation is much harder since the Ag NWs are almost straight) or else the Ag NW would break at very small strains; moreover, distributed rupture (including the break of nanowires and the dewelding) should be another reason for the large stretchability. Additionally, the dewelding allows for the sliding of the nanowires, which may also release the stresses at large strains, and such sliding has been observed by Wiley et al. [50].

Please cite this article in press as: C.F. Guo, Z. Ren, Mater. Today (2014), http://dx.doi.org/10.1016/j.mattod.2014.08.018

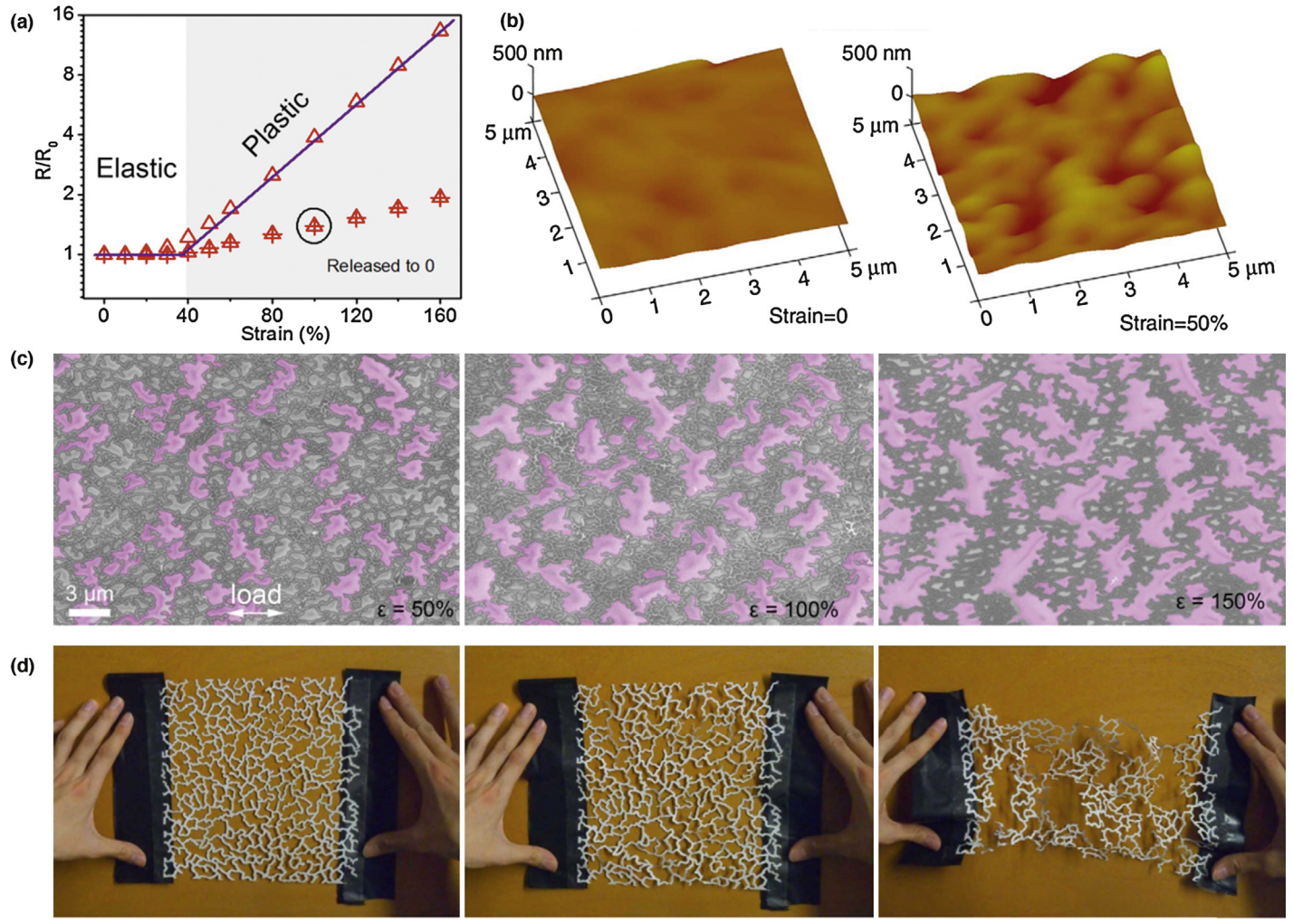

FIGURE 7

Out-of-plane deformation and distributed rupture. (a) The Au nanomesh deforms plastically at small strains and plastically at large strains. (b) Atomic force microscopy images of unstretched and stretched Au nanomesh supported on PDMS, showing out-of-plane deformation in the stretched Au nanomesh. (c) Au nanomesh/PDMS stretched at strains of 50%, 100% and 150%, showing that distributed cracks (filled with purple) are formed and the crack size increases with increasing strain. (d) A demonstration showing that the pre-cut mesh made of paper is much more stretchable. Figures reprinted with permission from Ref [44], copyright Nature Publishing Group 2014.

Criteria for evaluating FTEs

The optical transmittance and electrical sheet resistance of the metal networks have been the focus of many endeavors, but we suggest that transmittance and sheet resistance, or σ_{dc}/σ_{op}, is not sufficient for evaluating the performances of an FTE. Several other properties should also be considered depending on the application.

Flexibility is a crucial property of FTEs used in flexible devices and it has been studied in part of the existing reports. However, most of the endeavors were focused on bending, which causes only small strains far less than 10%. Among various models of deformation including bending, twisting, folding, and stretching, stretching is the most demanding and directly gives the value of strain. It is therefore more critical and more scientific to use stretching as a standard test. Two aspects are critical: the change of resistance (R/R_0) for one-time stretching and for strain cycling (i.e. fatigue, will be discussed hereinafter). For example, our Au nanomeshes exhibited the best properties among the metal FTEs. The R/R_0 was 13.3 with a one-time stretching of 160% [44], and only four at a 100% strain. The best result for Ag NW networks was from GO-soldered Ag NWs, for which R/R_0 was 20 at a strain of 100% [40].

Fatigue is also critical, which can often be seen in strain cycling, determines durability and whether an FTE can be used in actual applications for a long time. For example, normalized R/R_0 increased by 32% for the Au nanomesh stretched for 1000 cycles between 0 and 50% strain (or increased 19% for 100 cycles between 0 and 100% strain), but a 41% increase was observed for GO-soldered Ag NW composite stretched to 40% for 100 cycles (extracted from the data in Ref [40]), indicating that the former has much smaller fatigue effect and better durability.

Haze is also an important parameter for transparent conducting electrodes, which is defined as the ratio of forward scattered light to all transmitted light [51]. For example, for commercial ITO films, haze is often listed in the product specifications. Some devices such as liquid crystal displays require low haze in order to offer a higher definition. But there are also some devices like solar cells which do not have a rigid requirement of haze. Hu et al.

Please cite this article in press as: C.F. Guo, Z. Ren, Mater. Today (2014), http://dx.doi.org/10.1016/j.mattod.2014.08.018

conducted a systematic study on the haze of Ag NW networks, finding that coarser NWs lead to higher haze [51]. Haze is also related to transmittance. Typically, lower haze is observed for Ag NW networks with a larger transmittance [21,34]. In addition, haze is expected to be related to the surface roughness of the FTEs. Generally speaking, low haze is desired for many applications.

Surface roughness is another important parameter. Lower surface roughness allows for strong bonding and easier post processing, and contributes to high performance of the devices. Solution processed Ag NW networks often exhibit high roughness due to the fact that the Ag NWs are not strictly in the same film plane. The slanting nanowires can be easily removed and may also lead to shortcut of front and back electrodes for some thin devices. Roughness is not significantly improved by applying welding processes including annealing, surface coating, or light illumination. However, there have been several ways to reduce the surface roughness of Ag NW networks. Hu et al. showed that with mechanical pressing, the surface roughness decreased from 110 nm to 47 nm [21]. Lu et al. successfully decreased roughness from 75 nm to 1.27 nm by burying the Ag NWs into polymer [37]. It is expected that smaller surface roughness may help to get a lower haze due to the weaker light scattering, although systematic studies and solid evidence have not yet been reported. An example might support this point: from our atomic force microscopy analysis, the Au nanomesh electrodes made by grain boundary lithography with a T of 83% and R_{sh} of 21 Ω/□ have a root-mean-square surface roughness R_q of only 8.8 nm, and corresponding haze is less than 4%. That means interconnects made by top-down processes (which can be regarded as a planer film with many holes) are more desired to achieve a low surface roughness. Note that the nanotrough networks, although being made by the top-down process, take the shape of electrospun polymer webs so that the surface roughness is higher (R_q = 141 nm) [42], and the value is close to that of metal NW networks [21].

Adhesion between the metal network and the elastomeric substrate is also very important for FTEs. To get a good stretchability, a suitable adhesion is required for the distributed rupture to occur. Either too good or too poor adhesion results in reduced stretchability. For an extreme case, when adhesion is zero (similar to the free-standing case), by elongating to a small strain, a Au nanomesh will break into two halves instead of forming distributed ruptures [44]. The detailed effect of adhesion on flexibility will be systematically discussed in a future paper. Adhesion also affects the durability of an FTE in devices like a touch screen. For Ag NW networks, a considerable part of NWs is not strongly adherent to the substrate, thus the suspending NWs are easy to detach. By contrast, metal interconnects made by top-down methods like Au nanomeshes are more adhesive to the substrate.

Stabilities including thermal and chemical stabilities should also be considered to be important. Typically, for thermal and chemical stabilities, Au is better than Ag, and Cu is the worst. Au does not have any oxidation problem and is therefore chemically stable in air and most of the acidic conditions. However, Au reacts with Si, forming a eutectic compound at ~300°C, therefore annealing Au FTEs on a Si substrate over 300°C should be avoided. Au networks are also proven to be thermally stable up to 500°C [44]. By contrast, Ag and Cu nanostructures cannot withstand high temperature annealing. Ag networks will be oxidized at 200°C while Cu will be slowly oxidized at ~80°C or even at room temperature [16,33,42]. Moisture accelerates the erosion of Cu [42]. However, a surface protective layer may effectively protect the Cu NWs from oxidation and other chemical erosions [33]. Therefore, Cu can still be a promising electrode material due to the lower price.

Table 1 compares different types of metal network FTEs regarding transmittance, sheet resistance, surface roughness, haze, stability, flexibility and fatigue. Briefly, the interconnects made by top-down method perform better. The nanotrough networks exhibit the best opto-electrical properties, while the Au nanomeshes exhibit the best properties of haze, roughness, and mechanical properties.

Some other materials including CNT, graphene, oxide NWs, and conducting organic materials (e.g. PEDOT:PSS) have also been developed as FTEs [2,52–55]. However, these materials do not exhibit excellent photoelectrical properties. Typically, CNT films have a R_{sh} of hundreds Ω/□ @ T = 79%, which is insufficient for many photoelectronic applications. However, the superstretchability (up to 150%) together with negligible fatigue when cycled at a 25% tensile stain for more than 10,000 cycles allow for applications with superflexibility such as tactile sensors [2]. Graphene sheets have good transmittance, but the sheet resistance is typically larger than 100 Ω/□. Graphene sheets are also stretchable (up to 30%) [53], but not as good as metal NW or CNT networks. Graphene may present advantages in haze, surface roughness, and adhesion. Other materials like oxide NW and organic FTEs are not highly conducting such that their applications are still quite limited. However, organic transparent conductors can mix with CNT or metal NW networks to improve the conductivity and to reduce the surface roughness.

Applications

The metal FTEs have many potential applications in such as liquid crystal displays (LCDs), touch screens, solar cells, OLED and electronic skins. For different applications, the requirements of transmittance, sheet resistance, flexibility, and other properties might differ. For example, touch screens often require a R_{sh} of 100–1000 Ω/□, a T of over 85% together with a low haze, while solar cell applications prefer a R_{sh} of <20 Ω/□ and T > 90% but no consideration of haze.

Guo et al. first used nanoimprinted metal grids in organic solar cells based on poly(3-hexylthiophene) (P3HT) and phenyl-C61-butyric acid methyl ester (PCBM), with efficiency comparable to those using ITO electrodes [19]. However, the flexibility of the solar cells was not studied. The solution processed Ag NW networks were then applied to replace the metal grids, and the P3HT/PCBM cells with Ag NW network electrode demonstrated 19% higher short circuit current, but ~10% lower efficiency due to much lower fill factor as shown in Fig. 8a [16]. Similar results were found for solar cells with mechanically pressed Ag NW network electrodes [23]. Metal NW composite electrodes were more extensively studied in solar cells, showing improved efficiency quite close to those using ITO electrodes [56–58]. For example, with a Ag NW-polymer composite electrode, the power conversion efficiency of P3HT/PCBM cells was comparable to control devices with ITO electrodes, while the devices were much more flexible and can be bent to a maximum 8% strain with negligible damage to device efficiency (Fig. 8b) [56]. Metal FTEs may also be applied in

Please cite this article in press as: C.F. Guo, Z. Ren, Mater. Today (2014), http://dx.doi.org/10.1016/j.mattod.2014.08.018

TABLE 1

The properties of several types of metal network FTEs.[a] Other conductor like carbon nanotube films and graphene sheet are also displayed as references

FTE	T	R_{sh} ($\Omega/\square$)	Roughness (R_q)	Haze	Thermal stability	Bending fatigue	One-time stretchability	Stretching fatigue
Ag NW network annealed	85% [16] 89% (long NWs) [25]	10 [16] 9 (long NWs) [25]	110 nm [21]	12% @ T = 78% (60 nm NWs), 28%@T = 72% (150 nm NWs) [51]	R start to increases @ 200°C for >20 min [16]	R is stable after 10,000 bends @ r = 2 mm (long NWs) [25]	–	R increases ~70% after 10 strain cycles (0–10% strain) [24]
Ag NW network (plasmonic welding) [22]	95%	580	–	–	–	–	–	–
Ag NW network (washed and spayed) [24]	94.1%	12.4	–	–	–	–	–	R increase 23% after 10 cycles with 0–10% ε
GO-soldered Ag NW network [40]	88%	14	–	–	–	$\Delta R_{sh} < 3\%$ after 12,000 bends	$R/R_0 \sim 20$ @ ε = 100%	ΔR = 41% @ ε = 40% after 100 cycles
Au nanotrough network [42]	94%	7.5	141	–	Good (R is stable at 120°C)	$\Delta R \sim 0$ with 10,000 bends @ r = 10 mm	$\Delta R_{sh} \sim 40\%$ @ ε = 50%	–
Au nanomesh [44]	82.5%	21	8.8	~4% @ T = ~80%	Good (R does not increase at 500°C)	$\Delta R \sim 70\%$ after 500 bends @ $r \ll 1$ mm	$\Delta R_{sh} = 0$ @ ε = 80%, or 2.2 @ ε = 160%	ΔR = 30% with 1000 cycles @ ε = 50%, or 19% with 100 cycles @ ε = 100%
Cu NW network	94.4% [33]	60 [33]	–	<1% @ T = 94% [33]	$R/R_0 > 10$ after 5 D in air [33]	$\Delta R \sim 0$ after 1000 bends, r = 2.5 mm [30]	–	–
Cu-Ni (54%) NW networks [33]	84.3%	60	–	~3% @ T = 84%	Good (stable at 85°C)	–	–	–
Spray-coated CNT film [2]	79%	328	–	–	–	–	ΔR = 5 @ ε = 150%	Negligible increase of R after 12,500 stretching cycles to 25%
Graphene [53]	76.9% @ 550 nm	>280	–	–	–	R increases ~10 times when bent to 1 mm	R increases >10 times when stretched to 30%	R has a small increase after 3 stretching cycles to 6%

[a] *Note*: $\Delta R = (R - R_0)/R_0$, $\Delta R_{sh} = (R_{sh} - R_{sh0})/R_{sh0}$, r presents bending radius, and ε presents strain. Some data are extracted from the plots in references.

Please cite this article in press as: C.F. Guo, Z. Ren, Mater. Today (2014), http://dx.doi.org/10.1016/j.mattod.2014.08.018

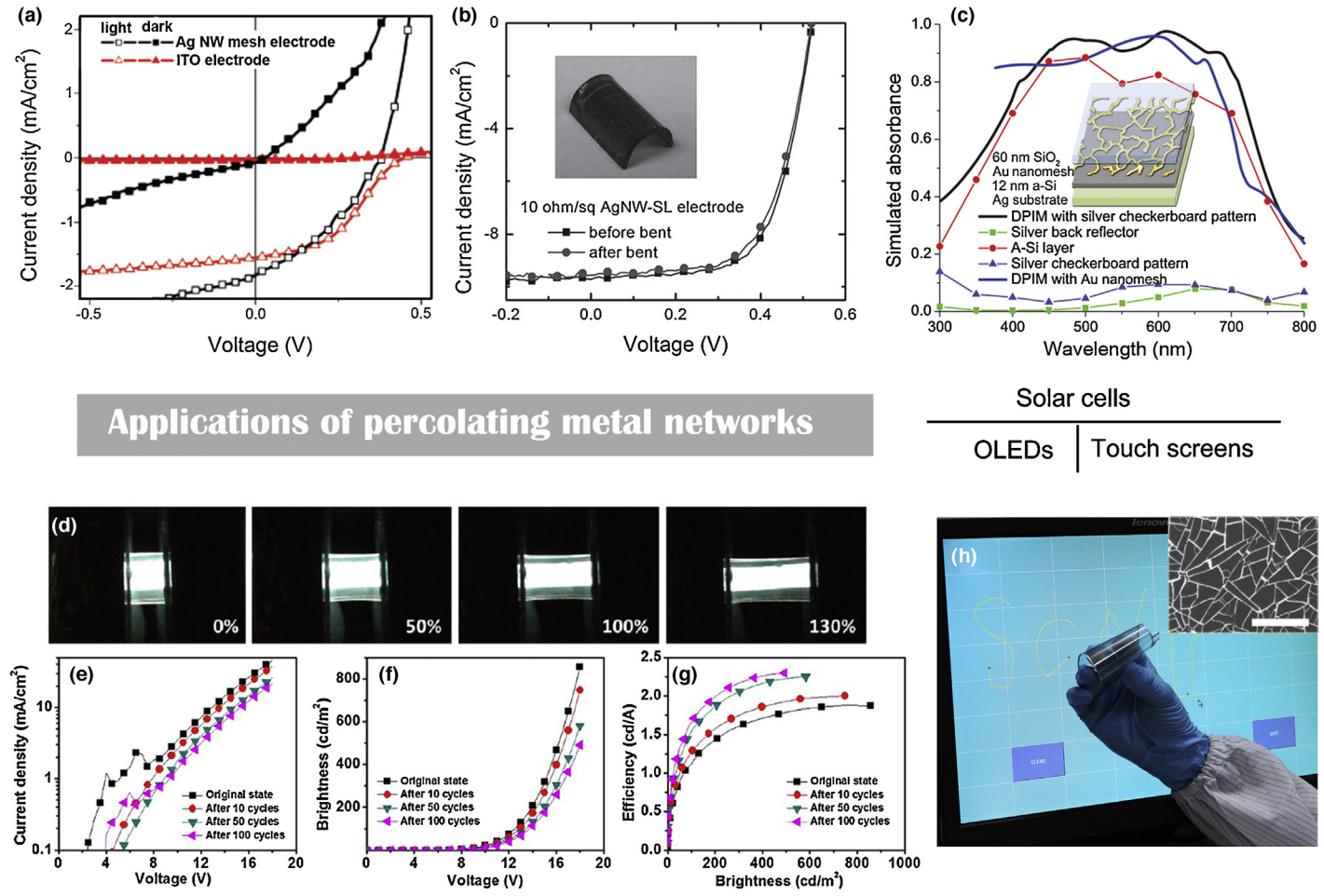

FIGURE 8

Applications of percolation metal network FTEs in solar cells, OLEDs and touch screens. (a) *I–V* characteristics of the first organic solar cell using Ag NW network, showing higher short circuit current but smaller fill factor compared with the cell using ITO electrode. (b) A flexible organic solar cell based on stacked Ag NW-polymer composite electrode, no significant change of efficiency is seen when the cell is bent. (c) Absorbance of ~10 nm a-Si solar cells using dielectric/perforated metal film/insulator/metal (DPIM) structures. The simulated absorbance is close with periodic or random Au nanomesh as the front electrode. (d) Stretchable OLED using GO-soldered Ag NW networks. (e–g) Change of current density, brightness, and efficiency of the OLED after stretched to 20% for different number of cycles. (h) A demonstration of using the crack-templated Ag network as the electrode for flexible touch screen. Inset is a SEM image of the crack-templated Ag network. Scale bar is 50 μm. Figures reprint with permission from Ref [16] (panel a) copyright American Chemical Society 2008, Ref [56] (panel b) copyright Wiley VCH 2011, Ref [59] (panel c) copyright Nature Publishing Group 2014, Ref [40] (panels c–g) copyright American Chemical Society 2014, and Ref [45] (panel h) copyright Wiley VCH 2014.

inorganic solar cells. Simulations indicated that the Au nanomesh made by grain boundary lithography as the front electrodes of ultra-thin amorphous Si (~10 nm) solar cells plays two important roles: acting as a transparent conducting electrode, and increasing absorbance in Si in a broad range (close to 90% in the wavelength range of 400–700 nm), as shown in Fig. 8c [59]. The high absorption effect is unique for the Au nanomeshes; other metal networks have larger and inhomogeneous mesh size and may not contribute to such an electromagnetic response.

For OLED applications, metal networks present several advantages over ITO films [18]. With Ag or Au network electrodes, there is no device degradation induced by indium diffusion, and we can select metals with high work function (e.g. Au) for highly efficient hole injection into the organic semiconductor [18]. More importantly, the devices can be flexible. Lee et al. demonstrated highly flexible metal conductor LED circuits with ultralong Ag NW networks [25]. Pei et al. demonstrated fully stretchable white OLEDs for the first time, employing the GO-soldered Ag NW network as both the anode and the cathode. The OLED can survive after one-time elongation up to 130% (Fig. 8d), or 100 stretching cycles between 0 and 40% strain (Fig. 8e–g) [40]. This result proves that the percolating metal networks can serve as the electrode for stretchable photoelectronics.

There have been several demonstrations in touch screens, by using solution processed Ag NW networks or crack-templated Ag interconnects (Fig. 8h) [25,45]. Touch screens are widely used in smart cell phones and tablet computers, and create a huge market. Flexible cell phones are on the way but people still need to find cost-effective FTEs to replace ITO films. The percolating metal networks may defeat ITO films and dominate this area.

The large stretchability of metal network FTEs may also be potentially useful in bioscience. For some tests or monitoring in body, the electrodes need to be much more flexible to comply with the motion of tissues or organs and be compatible with the bio-environment. Au nanomeshes might be a potential selection allowing for good flexibility, percolating of liquid, as well as

Please cite this article in press as: C.F. Guo, Z. Ren, Mater. Today (2014), http://dx.doi.org/10.1016/j.mattod.2014.08.018

stimulating with or monitoring optical/electrical signals. Epidermal electronics with flexible metal electrodes have already been demonstrated [60]. However, there have been few attempts for biotest in body with flexible metal FTEs. This will be a new but challenging area.

Concluding remarks and perspective

This review briefly discusses the state-of-the-art of metal FTEs. How to decrease or even eliminate the wire–wire junction resistance or construct fully interconnected networks is critical for this community. For transmittance and sheet resistance, metal FTEs are already comparable or even better than the commercial ITO films, while exhibiting much better flexibility that allows devices to be bent or even stretched. Compared with solution processed metal nanowire networks, metal interconnects made by top-down methods exhibit better overall properties. We point out that the flexible elastomeric substrate plays important roles in achieving large stretchability. We also suggest that several other properties, including stretchability, strain fatigue, haze, adhesion, surface roughness, and thermal stability, although have not yet been intensively investigated, are also important to FTEs depending on the application. Future works should consider part or all of such properties regarding targeted applications. The high performance FTEs might be used in flexible electronics and soft machines in which the mechanical properties of a soft/stiff interface are critical. Specifically, for integrated devices built on FTE/elastomeric substrate, although the FTEs can be very flexible, the islands of stiff materials (the devices) may debond at small strains [61,62]. Such issues deserve much more investigation. Cracking and failure of the metal networks under large strain are also of great interest. This area needs a lot of studies and may have a significant impact on the next generation of photoelectronic industry in which flexible devices may boom in the near future.

Acknowledgement

This work is funded by the US Department of Energy under Contract Number DOE-DE-FG02-13ER46917/DE-SC0010831.

References

[1] D.J. Lipomi, Z. Bao, Energy Environ. Sci. 4 (9) (2011) 3314–3328.
[2] D.J. Lipomi, et al. Nat. Nanotechnol. 6 (12) (2011) 788–792.
[3] W. Hu, et al. Appl. Phys. Lett. 102 (8) (2013) 083303.
[4] L. Hu, H. Wu, Y. Cui, MRS Bull. 36 (10) (2012) 760–765.
[5] C. Keplinger, et al. Science 341 (6149) (2013) 984–987.
[6] D.S. Hecht, L.B. Hu, G. Irvin, Adv. Mater. 23 (13) (2011) 1482–1513.
[7] P.P. Edwards, et al. Dalton Trans. 19 (2004) 2995–3002.
[8] P. Gutruf, et al. NPG Asia Mater. 5 (9) (2013) e62.
[9] M.W. Rowell, et al. Appl. Phys. Lett. 88 (23) (2006) 233506.
[10] L. Hu, D.S. Hecht, G. Grüner, Nano Lett. 4 (12) (2004) 2513–3251.
[11] D. Zhang, et al. Nano Lett. 6 (9) (2006) 1880–1886.
[12] J. Chen, et al. Adv. Mater. 20 (3) (2008) 566–570.
[13] A. Kumar, C. Zhou, ACS Nano 4 (1) (2010) 11–14.
[14] P.E. Lyons, et al. J. Phys. Chem. Lett. 2 (24) (2011) 3058–3062.
[15] S. De, et al. ACS Nano 3 (7) (2009) 1767–1774.
[16] J.Y. Lee, et al. Nano Lett. 8 (2) (2008) 689–692.
[17] http://sscorning.en.ec21.com/ITO_Glass-1_3256926.html.
[18] M.-G. Kang, L.J. Guo, Adv. Mater. 19 (10) (2007) 1391–1396.
[19] M.-G. Kang, et al. Adv. Mater. 20 (23) (2008) 4408–4413.
[20] A. Tao, et al. Nano Lett. 3 (9) (2003) 1229–1233.
[21] L. Hu, et al. ACS Nano 4 (5) (2010) 2955–2963.
[22] E.C. Garnett, et al. Nat. Mater. 11 (3) (2012) 241–249.
[23] T. Tokuno, et al. Nano Res. 4 (12) (2011) 1215–1222.
[24] J. Lee, et al. Small 9 (17) (2013) 2887–2894.
[25] J. Lee, et al. Nanoscale 4 (20) (2012) 6408–6414.
[26] S.M. Bergin, et al. Nanoscale 4 (6) (2012) 1996–2004.
[27] R.M. Mutiso, et al. ACS Nano 7 (9) (2013) 7654–7663.
[28] R.M. Mutiso, K.I. Winey, Phys. Rev. E 88 (3) (2013) 032134.
[29] J. van de Groep, P. Spinelli, A. Polman, Nano Lett. 12 (6) (2012) 3138–3144.
[30] A.R. Rathmell, et al. Adv. Mater. 22 (32) (2010) 3558–3563.
[31] S. Ye, et al. Small 10 (9) (2014) 1771–1778.
[32] A.R. Rathmell, J.W. Benjamin, Adv. Mater. 23 (41) (2011) 4798–4803.
[33] A.R. Rathmell, et al. Nano Lett. 12 (6) (2012) 3193–3199.
[34] H. Guo, et al. Sci. Rep. 3 (2013) 2323.
[35] Z. Huo, et al. Nano Lett. 8 (7) (2008) 2041–2044.
[36] A. Sánchez-Iglesias, et al. Nano Lett. 12 (12) (2012) 6066–6070.
[37] X.-Y. Zeng, et al. Adv. Mater. 22 (40) (2010) 4484–4488.
[38] W. Gaynor, et al. Adv. Mater. 23 (26) (2011) 2905–2910.
[39] Y. Liu, Q. Chang, L. Huang, J. Mater. Chem. C 1 (17) (2013) 2970–2974.
[40] J. Liang, et al. ACS Nano 8 (2) (2014) 1590–1600.
[41] I.K. Moon, et al. Sci. Rep. 3 (2013), http://dx.doi.org/10.1038/srep01112.
[42] H. Wu, et al. Nat. Nanotechnol. 8 (2013) 421–425.
[43] C.F. Guo, et al. Small 9 (14) (2013) 2415–2419.
[44] C.F. Guo, et al. Nat. Commun. 5 (2014) 3121.
[45] B. Han, et al. Adv. Mater. 26 (6) (2014) 980.
[46] C.F. Guo, et al. Nano Energy 8 (2014) 110–117.
[47] S.P. Lacour, et al. Appl. Phys. Lett. 88 (20) (2006) 204103.
[48] I.M. Graz, et al. Appl. Phys. Lett. 94 (7) (2009) 071902.
[49] T. Li, et al. J. Mater. Res. 20 (12) (2005) 3274–3277.
[50] J. Wu, et al. Nano Lett. 13 (6) (2013) 2381–2386.
[51] C. Preston, et al. Nano Res. 6 (7) (2013) 461–468.
[52] M. Kaempgen, G.S. Duesberg, S. Roth, Appl. Surf. Sci. 252 (2) (2005) 425–429.
[53] K.S. Kim, et al. Nature 457 (7230) (2009) 706–710.
[54] S. Huang, et al. NPG Asia Mater. 6 (2) (2014) e86.
[55] J. Ouyang, ACS Appl. Mater. Interfaces 5 (24) (2013) 13082–13088.
[56] Z. Yu, et al. Adv. Mater. 23 (38) (2011) 4453–4457.
[57] R. Zhu, et al. ACS Nano 5 (12) (2011) 9877–9882.
[58] D.-S. Leem, et al. Adv. Mater. 23 (38) (2011) 4371–4375.
[59] C.F. Guo, et al. Light: Sci. Appl. 3 (2014) e161, http://dx.doi.org/10.1038/lsa.2014.42.
[60] D.-H. Kim, et al. Science 333 (6044) (2011) 838–843.
[61] Z. Suo, MRS Bull. 37 (03) (2012) 218–225.
[62] J.-Y. Sun, et al. J. Appl. Phys. 113 (22) (2013) 223702.

Please cite this article in press as: C.F. Guo, Z. Ren, Mater. Today (2014), http://dx.doi.org/10.1016/j.mattod.2014.08.018